Synthesis of Silica-Based Solid-Acid Catalyst Material as a Potential Osteochondral Repair Model *In Vitro*

Rui-Min Long[1†], Yan Jiang[2†], Jia-Qi Guo[1], Gang Ren[2], Xian-Xin Guo[1], Xue Xie[1], Yue Wu[1], Rui-Da Yan[1], Zi-Zhen Lin[1], Shi-Bin Wang[2,3,4] and Yuan-Gang Liu[1,3,4]*

[1]College of Chemical Engineering, Huaqiao University, Xiamen, China, [2]College of Materials Science and Engineering, Xiamen, China, [3]Institute of Pharmaceutical Engineering, Huaqiao University, Xiamen, China, [4]Fujian Provincial Key Laboratory of Biochemical Technology, Xiamen, China

For osteochondral damage, the pH value change of the damaged site will influence the repair efficacy of the patient. For better understanding the mechanism of the acid-base effect, the construction of *in vitro* model is undoubtedly a simple and interesting work to evaluate the influence. Here, a novel porous silica-based solid-acid catalyst material was prepared by additive manufacturing technology, exhibiting improved eliminating effects of the residue. SEM, FTIR, and TGA were used to characterize the morphology, structure, and thermal stability of the synthesized 3D material. The reaction between 4-methoxybenzyl alcohol and 3, 4-dihydro-2*H*-pyran was used as a template reaction to evaluate the eliminating performance of the 3D porous material. Solvents were optimized, and three reaction groups in the presence of 3D SiO_2, 3D SiO_2-SO_3H, and 3D SiO_2-NH-SO_3H, as well as one without catalyst, were compared. In addition, in consideration of the complicated situation of the physiological environment *in vivo*, universality of the synthesized 3D SiO_2-NH-SO_3H catalyst material was studied with different alcohols. The results showed that the sulfonic acid-grafted 3D material had excellent catalytic performance, achieving a yield over 95% in only 20 min. Besides, the catalyst material can be recycled at least 10 times, with yields still higher than 90%. Such a solid catalyst material is expected to have great potential in additive manufacturing because the catalyst material is easy-recyclable, renewable and biocompatible. The 3D material with connective channels may also be utilized as an *in vitro* model for environment evaluation of osteochondral repair in the future.

Keywords: solid-acid catalyst material, 3D printing, SiO_2, osteochondral repair, *in vitro* evaluation

INTRODUCTION

For decades, many people suffer from various bone and cartilage damages such as arthritis. To treat these diseases, tissue engineering provides a promising and alternative method in orthopedic surgery and biomedical engineering (Wei et al., 2021a). For example, Wei et al. fabricated a 3D printed polycaprolactone scaffold modified by insulin-releasing PLGA nanoparticles for osteochondral repair, and the results indicate that both of the *in vitro* and *in vivo* studies show that the insulin-releasing scaffolds significantly improve the osteogenic differentiation of rabbit bone mesenchymal stem cells and the proliferation of

chondrocytes, and further improve the repair of cartilage and subchondral bone after 8- and 12-weeks implantation in rabbit osteochondral defects (Wei et al., 2021b). However, several factors have great influence on tissue regeneration, for example, such as the degradation of the biomaterials will result in the acid-base concentration change at the treatment site (Li et al., 2021; Xue et al., 2021), and the enrichment and diffusion of calcium ions could promote neovascularization and repair of the critical defect (Xing et al., 2021). Thus, to understand the influence of these factors is an important issue for bone and cartilage repair. *In vitro* model provides an indirect and convenient platform to assess the repair effect and scrutinize different molecular and possible therapeutic targets for better understanding the mechanisms and osteoarthritis therapeutics (Hopkins et al., 2021; Singh et al., 2021). Consequently, The aim of this work is to establish an *in vitro* model to evaluate the effect of acid-base by preparing a novel porous silica-based solid-acid catalyst material using additive manufacturing technology which may exhibit improved eliminating effects. To prepare the model, in the synthesis of some complex compounds, molecule intermediates often carry multiple functional groups, and sometimes, these functional groups react with other reactants before the intended product(s) can be formed. Therefore, protecting some functional groups of the molecule from reaction is necessary, while leaving other functional groups free to participate in the reaction (Rajkumari et al., 2017). One important example is the protection of hydroxyl groups. Until now, many ways have been discovered to achieve alcohol protection. Among these methods, ether-forming protection of hydroxyl groups (reaction of an alcohol with 3,4-dihydro-2*H*-pyran) is considered the most popular and convenient solution (Kumar et al., 2014; Khder et al., 2018). This is because, first, the protective agent is easier to prepare than other protective agents. Further, the corresponding ether pair reaction conditions and some reagents used, such as the format reagent, hydride, strong alkali, and other organometallic reagents, have good stability (Azzena et al., 2018). Lastly, many kinds of catalysts have been reported for tetrahydropyranylation of alcohols, including ionic liquids (Rafael et al., 2001), silica chloride (Ravindranath et al., 2001), Al(OTf)$_3$ (Williams et al., 2010), silica sulfonic acid (Shimizu et al., 2004), and modified zeolites (Narender et al., 2010; Shin et al., 2017). However, many of them have disadvantages, such as low efficiency, instability, harsh reaction conditions, and an inability to be recycle. Preparing catalysts free from these disadvantages is an important research direction (Nakhaei et al., 2019; Sajjadifar et al., 2019). According to previous work, advanced continuous porous structures help control and increase the distribution of catalytically active components, enhancing catalytic performance (Stuecker et al., 2004; Ludwig et al., 2018). However, traditional porous materials are obtained by a template method and vapor deposition, as well as others, and suffer from long preparation cycles and complicated steps (Xintong and Chang-jun, 2017). Additive manufacturing technology, also called 3D printing, is a powerful tool for designing advanced structures (Wang et al., 2020). Silica is preferred as a carrier for its stability in most solvents, and Niknam and coworkers (Niknam et al., 2010) successfully prepared silica-bonded S-sulfonic acid (SBSSA) and employed it as a recyclable catalyst for the condensation reaction of aromatic aldehydes with 3-methyl-l-phenyl-5-pyrazolone. With continued catalyst development, Pourghasemi-Lati and colleagues (Pourghasemi-Lati et al., 2018) immobilized butane-1-sulfonic acid on magnetic Fe$_3$O$_4$@SiO$_2$ nanoparticles for the synthesis of 5-arylidine barbituric acids and pyrano [2,3-*d*] pyrimidine derivatives. In addition, silica-based biomaterials have been widely studied in bone and cartilage tissue engineering due to high mechanical stiffness, high biocompatibility, and special bioactivities including stimulating osteogenesis and angiogenesis by enhancing corresponding gene expressions (Li et al., 2000; Du et al., 2015; Ishikawa et al., 2018). For example, silica based inorganic/organic hybrids could promote collagen Type II, Sox9 and Aggrecan production from chondrocytes (Nelson et al., 2021) or have mechanically strong and elastic characteristics (Yu et al., 2021).

Here, a new silica carrier is described, fabricated by 3D printing and combined with advanced structural perspectives. Further, chemical modifications were carried out, introducing many sulfonic acid groups, and the catalyst material was applied to hydroxyl protection reactions as model test. In addition, in consideration of the complicated situation of the physiological environment *in vivo*, universality of the synthesized material was studied. The new material is anticipated to be utilized as an *in vitro* model for environment evaluation of osteochondral repair in the future.

EXPERIMENTS

Materials and Equipment

SiO$_2$ powder (industrial grade) was provided by Delu Hardware & Plastic Co., Ltd. Chlorosulfonic acid (99% purity) was supplied by Energy Chemical. Analytical grade chemicals, including sodium alginate, ethanol, trichloromethane, dichloromethane, 3, 4-dihydro-2*H*-pyran, (3-chloropropyl) triethoxysilane, diethylenetriamine, 1-hexanol, 1-octanol, 1-dodecanol, 1-hexadecanol, cyclohexanol, cyclohexanemethanol, 4-methoxybenzyl alcohol, 4-chlorobenzyl alcohol, 4-bromobenzyl alcohol, and 4-methylbenzyl alcohol, were all purchased from Aladdin or Sinopharm Chemical Reagent Co., Ltd. A 3D printer (Regenovo 3D Bio-Architect®-WS) was utilized to prepare the 3D model, and a furnace (Tianjin Zhong Huan, 1,600°C) was used for post-processing of the model.

Preparation of Porous SiO$_2$

SiO$_2$ powder was first dispersed in ethanol and, then, loaded in a syringe and installed on the 3D printer. Next, the porous silica structure was printed under a pressure of 0.5 MPa and speed of

SCHEME 1 | 3D SiO_2-SO_3H.
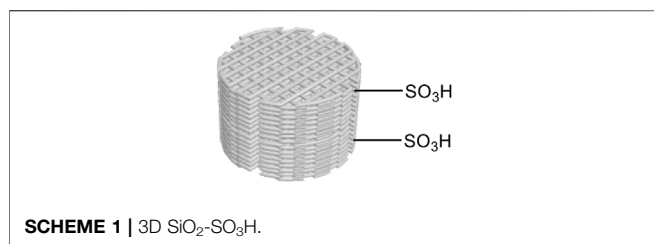
6 mm/s. Porous SiO_2 was obtained via a sintering process at 1,500°C. In the following research, two kinds of porous silica-based solid-acid catalysts were prepared: 3D SiO_2-SO_3H (catalyst 1) and 3D SiO_2-NH-SO_3H (catalyst 2).

Preparation of Porous Silica-Based Solid-Acid Catalyst 1

Three-dimensional SiO_2 was first activated by 15 ml of 30% H_2O_2 under 150°C to increase the number of hydroxyl groups. After drying, three pieces of 3D SiO_2 were mixed with chlorosulfonic acid (0.5 ml) and reacted in $CHCl_3$ (8 ml) at 0°C for 4 h. After drying in the vacuum drying oven, catalyst 1 (3D SiO_2-SO_3H, **Scheme 1**) was obtained.

Preparation of Porous Silica-Based Solid-Acid Catalyst 2

A schematic diagram of the preparation of 3D SiO_2-NH-SO_3H is presented in **Figure 1**. Briefly, the carrier was first activated by 15 ml of 30% H_2O_2 at 150°C to increase the number of hydroxyl groups (Díaz-Marta et al., 2018). Then, (3-chloropropyl)triethoxysilane (0.5 ml) was used to modify the surface of porous SiO_2, yielding the chlorine-modified porous carrier (3D SiO_2-Cl, Scheme 2 in **Figure 1**). To obtain more sulfonic acid groups, 3D SiO_2-Cl (three pieces) were put in a round-bottomed flask with diethylenetriamine (5 mmol), triethylamine (5.5 mmol), and DMF (10 ml) and reacted at 100°C for 12 h. After drying, the intermediate

product, with double terminal amino groups, was obtained (3D SiO_2-NH_2, Scheme 3 in **Figure 1**). Finally, three pieces of 3D SiO_2-NH_2 were mixed with chlorosulfonic acid (0.5 ml) in $CHCl_3$ (8 ml) for 4 h at 0°C, and then, catalyst 2 (3D SiO_2-NH-SO_3H, Scheme 4 in **Figure 1**) was obtained via drying in the vacuum drying oven.

## Catalytic Reaction of the 3D Porous Catalyst

Catalytic activity was investigated via the reaction between 4-methoxybenzyl alcohol (5 mmol) and 3, 4-dihydro-2*H*-pyran (5.5 mmol). To begin, different solvents (10 ml) were tested, to determine the most efficient one. Further, the material, obtained via direct sulfonation of activated SiO_2 (3D SiO_2-SO_3H), was compared with 3D SiO_2-NH-SO_3H. Under optimized solvent conditions in the presence of 3D SiO_2-NH-SO_3H, different alcohols were reacted with 3, 4-dihydro-2*H*-pyran, and product yields and corresponding reaction times were recorded.

Physiochemical Characterization

Scanning electron microscopy (SEM; Phenom Pro, Phenom-World Co., Ltd. Eindhoven, Netherlands) was used to observe the material micro-surface. Fourier transform infrared spectroscopy (FTIR; NICOLET IS 50, Thermo Fisher Scientific Co., Ltd. Massachusetts, United States) was utilized to determine whether the sulfonic acid group successfully grafted onto SiO_2. Thermogravimetric analysis (TGA; TGA-50, Shimadzu Co., Ltd. Kyoto, Japan) was also used to confirm the molecules were grafted on 3D SiO_2. Catalytic reaction products were characterized by FTIR and ^1H NMR spectroscopy (NMR; Advance III HD 500MHz, Bruker Technology Co., Ltd. New York, United States).

Cytotoxicity Test

C518 cells were seeded in a 96-well plate at a density of 5×10^3 cells per well and cultured for 24 h at 37°C. Then, the medium was removed, and cells were incubated with different concentrations of sample leaching solution (12.5, 25, 50, 100, and 200 μg/ml). Cell
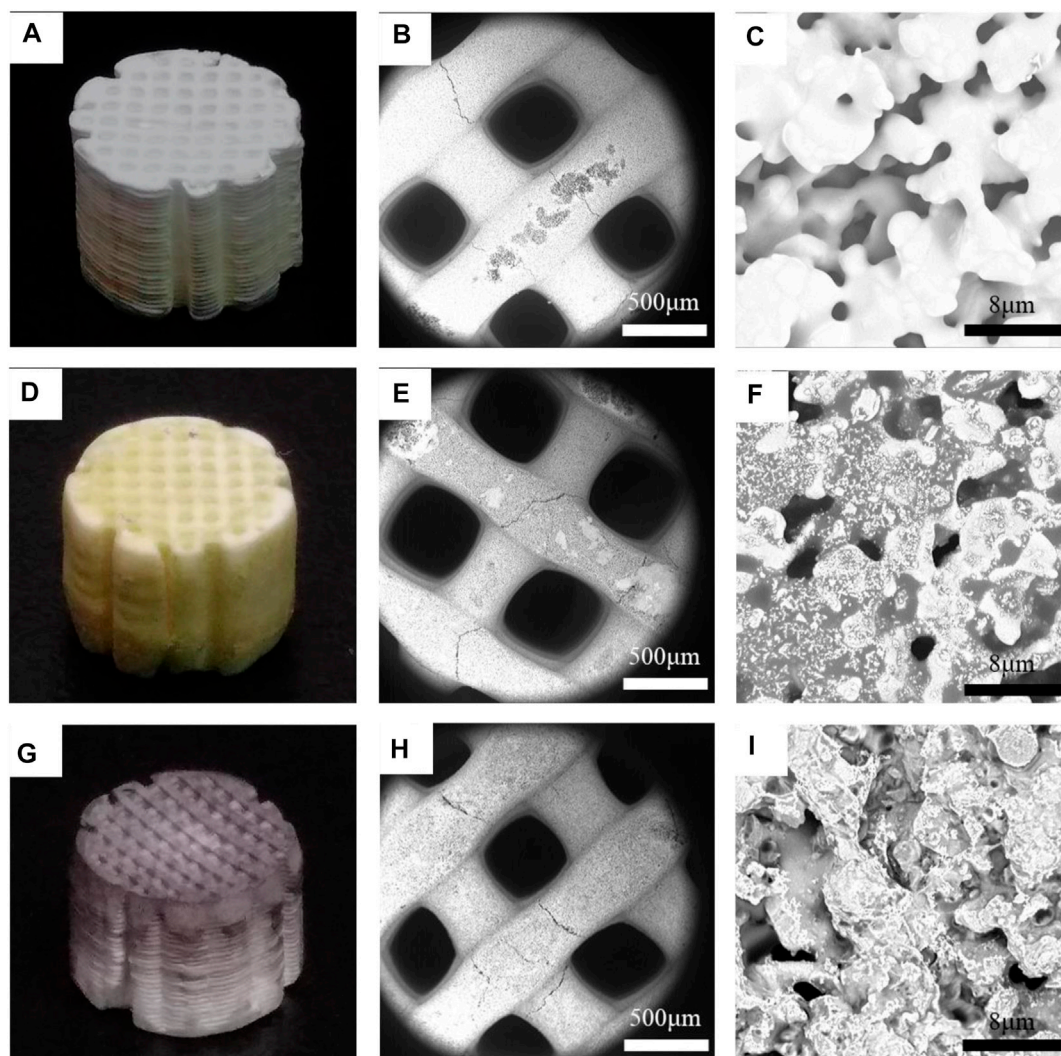

FIGURE 1 | Schematic of the 3D SiO_2-NH-SO_3H synthesis.
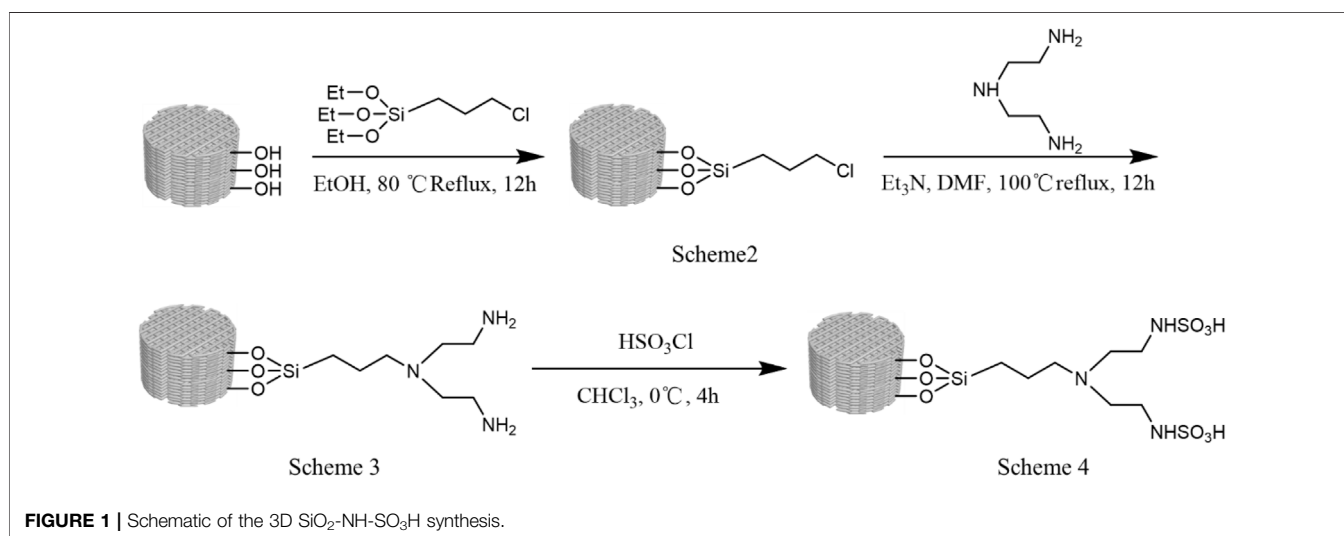
FIGURE 2 | Optical images of **(A)** 3D SiO$_2$, **(D)** 3D SiO$_2$-NH-SO$_3$H, and **(G)** 3D SiO$_2$-NH-SO$_3$H after one catalytic cycle. SEM images of **(B,C)** 3D SiO$_2$; **(E,F)** 3D SiO$_2$-NH-SO$_3$H; and **(H,I)** 3D SiO$_2$-NH-SO$_3$H after one catalytic cycle at different magnifications.

viability at 24 and 48 h was determined, respectively *via* CCK-8 assay according to the instructions provided by the manufacturer using a microplate reader under 450 nm (Spectrophotometer-1510, Thermo Fisher Scientific Co., Ltd. Massachusetts, United States). Cell viability rate was calculated according to the following formula: Cell viability (%) = (OD$_{sample}$ − OD$_{blank}$)/(OD$_{control}$ − OD$_{blank}$) × 100, where control means cells with fresh medium and blank is fresh medium.

RESULTS AND DISCUSSION

Three-dimensional SiO$_2$ was observed, together with fresh 3D SiO$_2$-NH-SO$_3$H, and 3D SiO$_2$-NH-SO$_3$H after one catalytic cycle in **Figure 2**. **Figures 2A**,D,G show optical images of as-prepared 3D SiO$_2$, fresh 3D SiO$_2$-NH-SO$_3$H, and 3D SiO$_2$-NH-SO$_3$H which catalysed the reaction of 1-octanol with 3, 4-dihydro-2H-pyran. Compared with the white colour of the

treated, blank 3D SiO$_2$, the surface of 3D SiO$_2$-NH-SO$_3$H was light yellow with some black dots, which were used for catalysing the reaction. The scanning electron microscope (SEM) images of as-prepared 3D SiO$_2$ (**Figures 2B**,C), fresh 3D SiO$_2$-NH-SO$_3$H (**Figures 2E**,F), and 3D SiO$_2$-NH-SO$_3$H after one catalytic cycle (**Figures 2H**,I) showed obvious differences. The micro-surface of the carrier and catalyst showed consequent holes, beneficial for introducing more sulfonic acid groups. Furthermore, grey parts existed on the smooth carrier surface, which could be a series of grafted molecules and sulfonic acid groups.

The presence of sulfonic acid groups on the surface of 3D porous silicon was confirmed by FTIR (**Figure 3**). The broad peak near 3,490 cm^{-1} was assigned to N-H stretching vibrations, while the peaks at 2,936 and 2,873 cm^{-1} were attributed to C-H stretching vibrations. The peak at 1,084 cm^{-1} arises from the stretching vibration of Si-O-Si, but due to the overlap of S=O and
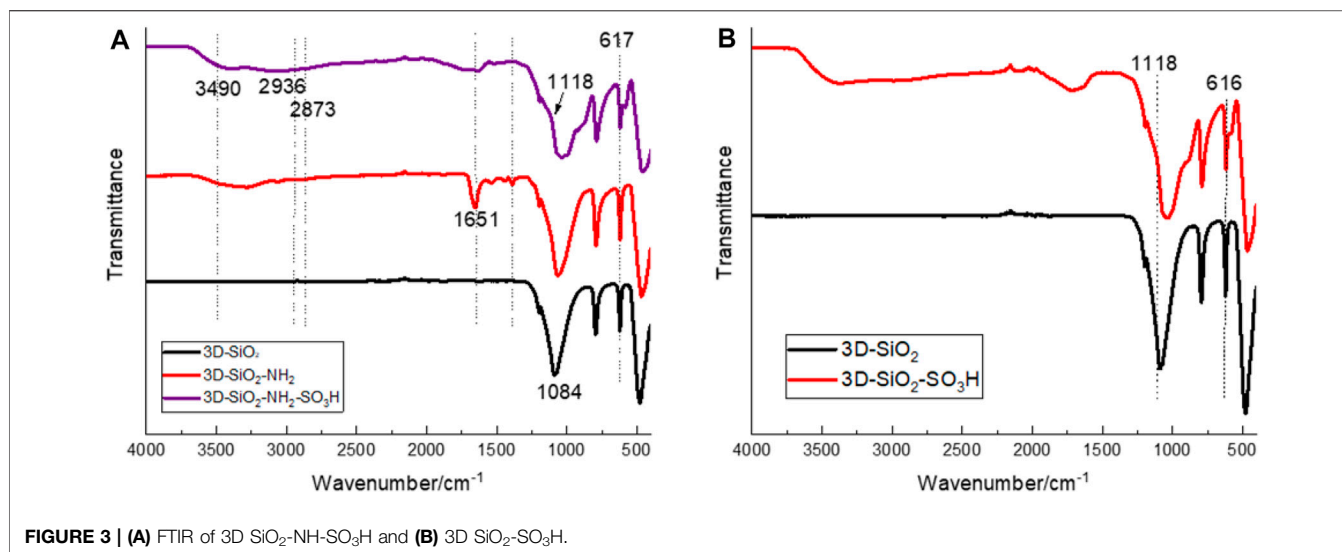
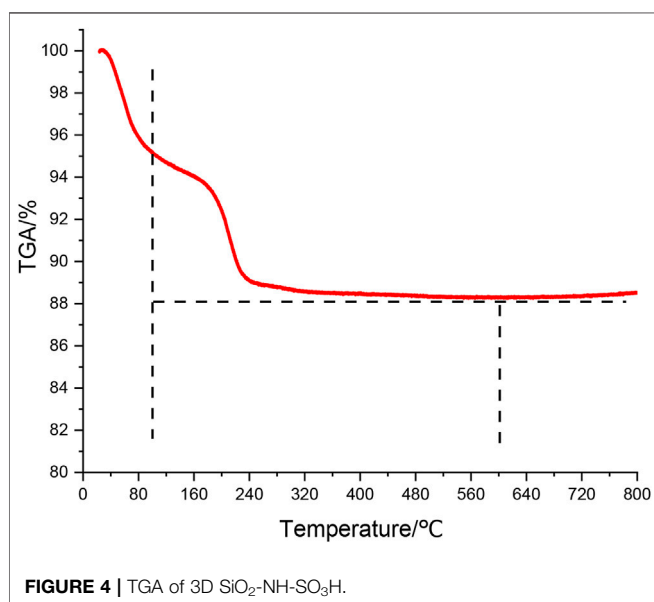**FIGURE 3 | (A)** FTIR of 3D SiO₂-NH-SO₃H and **(B)** 3D SiO₂-SO₃H.

FIGURE 4 | TGA of 3D SiO₂-NH-SO₃H.

TABLE 1 | Comparison of the best solvents for reaction in the presence of 3D SiO₂-NH-SO₃H.

Entry	Catalyst	Solvent	Yield/%
1	3D SiO₂-NH-SO₃H	—	86
2	3D SiO₂-NH-SO₃H	Acetone	87
3	3D SiO₂-NH-SO₃H	Acetonitrile	87
4	3D SiO₂-NH-SO₃H	Toluene	92
5	3D SiO₂-NH-SO₃H	Ethyl acetate	89
6	3D SiO₂-NH-SO₃H	Tetrahydrofuran	78
7	3D SiO₂-NH-SO₃H	Methylene chloride	96
8	—	Methylene chloride	—

Reaction conditions: 4-methoxybenzyl alcohol (5 mmol), 3, 4-dihydro-2H-pyran (5.5 mmol), and 3D SiO₂-NH-SO₃H (seven pieces), stirred at room temperature for 20 min.

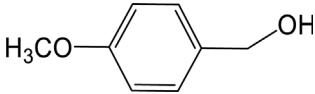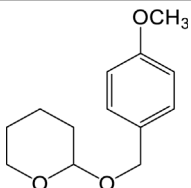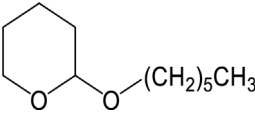**TABLE 2 |** Comparison of catalytic efficiency for different sulfonated catalysts.
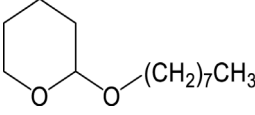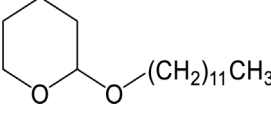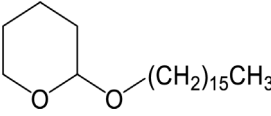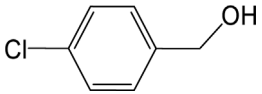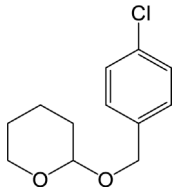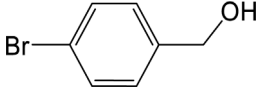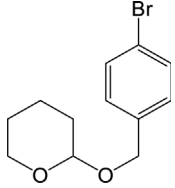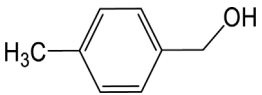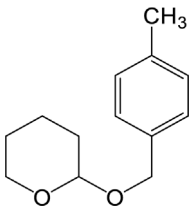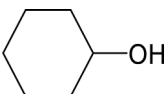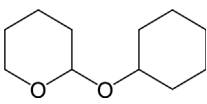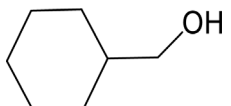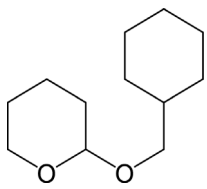
Entry	Catalyst	Time	Yield/%
1	3D SiO₂-NH-SO₃H (0.5 ml ClSO₃H/3 pieces)	20 min	96
2	3D SiO₂-SO₃H (0.5 ml ClSO₃H/3 pieces)	20 min	92
3	—	24 h	—
4	3D SiO₂	24 h	—

Reaction conditions: 4-methoxybenzyl alcohol (5 mmol), 3, 4-dihydro-2H-pyran (5.5 mmol), and 3D SiO₂ (1 piece), 3D SiO₂-SO₃H (1 piece), or 3D SiO₂-NH-SO₃H (1 piece) in CH₂Cl₂ (8 ml). The reaction was stirred at room temperature.

Si-O-Si characteristic peaks around 1,100 cm^{-1}, the half-peak at 1,118 cm^{-1} was considered to be the stretching vibration peak of S=O (Pourghasemi-Lati et al., 2018). In the low wavenumber region, some characteristic sulfonic acid peaks also overlapped with SiO₂, and the peaks at 617 and 616 cm^{-1} could be stretching vibrations of S-O.

TGA was also completed to determine the stability of the solid-acid catalyst material (**Figure 4**). The curve indicated that weight loss from room temperature to 100°C was a rapid, decreasing process, which may be mainly water evaporation. As the temperature continued to rise, no plateau was seen, which may indicate the material began to decompose. At about 600°C, the grafted molecules were completely decomposed.

To optimize reaction conditions for the synthesized material, we used the reaction of 4-methoxybenzyl alcohol and 3, 4-dihydro-2*H*-pyran as a template and explored the effect of different solvents on the catalytic yield in the presence of catalyst material (**Table 1**). In all solvents examined, methylene chloride showed the highest yield of 96% after 20 min. Furthermore, most of the non-polar solvents were promoting and exhibited better catalytic effects.

After choosing methylene chloride as the best solvent, catalyst 2 was compared with catalyst 1 by conducting catalytic

TABLE 3 | Catalytic effects of different alcohols under the action of 3D SiO$_2$-NH-SO$_3$H.

| Entry	Substrate	Time/min	Product	Yield/%
1	H$_3$CO—C$_6$H$_4$—CH$_2$OH	20		96
2	CH$_3$(CH$_2$)$_5$—OH	20		92
3	CH$_3$(CH$_2$)$_7$—OH	20		94
4	CH$_3$(CH$_2$)$_{11}$—OH	20		96
5	CH$_3$(CH$_2$)$_{15}$—OH	30		98
6	Cl—C$_6$H$_4$—CH$_2$OH	30		95
7	Br—C$_6$H$_4$—CH$_2$OH	20		96
8	H$_3$C—C$_6$H$_4$—CH$_2$OH	20		90
9	cyclohexanol	30		89
10	cyclohexylmethanol	30		94

Reaction conditions: alcohol (5 mmol), 3, 4-dihydro-2H-pyran (5.5 mmol), and 3D SiO$_2$-NH-SO$_3$H (10 pieces), stirred at room temperature.

FIGURE 5 | Recyclability of 3D SiO$_2$-NH-SO$_3$H.
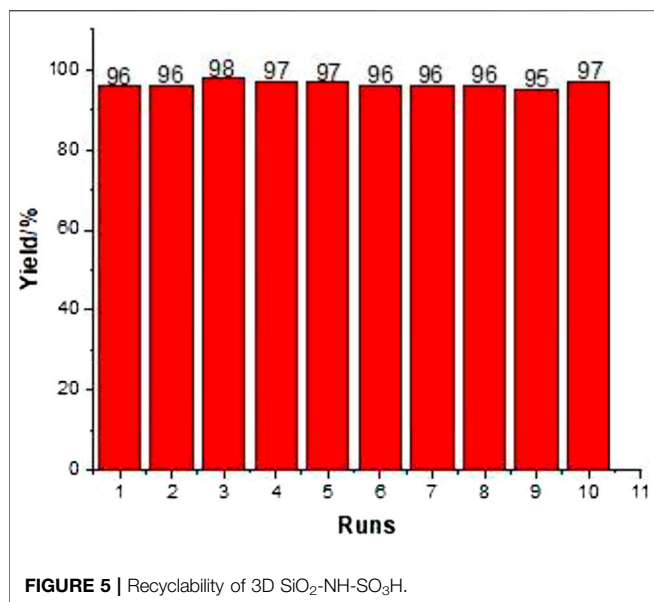
based solid-acid material had broad catalytic effects; many alcohol reactions were catalysed with high yields of 89% or more, with 1-hexadecanol (Entry 5) achieving a 98% yield (**Table 3**).

Lastly, the recyclability of 3D SiO$_2$-NH-SO$_3$H was investigated by the model reaction of 4-methoxybenzyl alcohol with 3, 4-dihydro-2*H*-pyran (**Figure 5**), demonstrating that the material could be used at least 10 times, while still achieving high catalytic yields. Other research also focuses on the reusable behaviour of SiO$_2$ catalyst (Kamble et al., 2021).

Meantime, in consideration of the new material is anticipated to be utilized as an *in vitro* model for osteochondral repair in the future work, the cytobiocompatibility is important because for the future evaluation, the cells must be seeded into the 3D scaffold. Thus the cytotoxicity test was performed using C518 cells as osteochondral model cell. As can be seen in **Figure 6**, both 3D SiO$_2$ and 3D catalyst exhibit excellent cell viability at different concentrations at 24 h, while at 48 h, the material shows limited cytotoxicity (<80%) only at high concentration (200 µg/ml), which indicates that the material is suitable for

FIGURE 6 | Cytotoxicity test of the materials **(A)**: 24 h; **(B)**: 48 h.
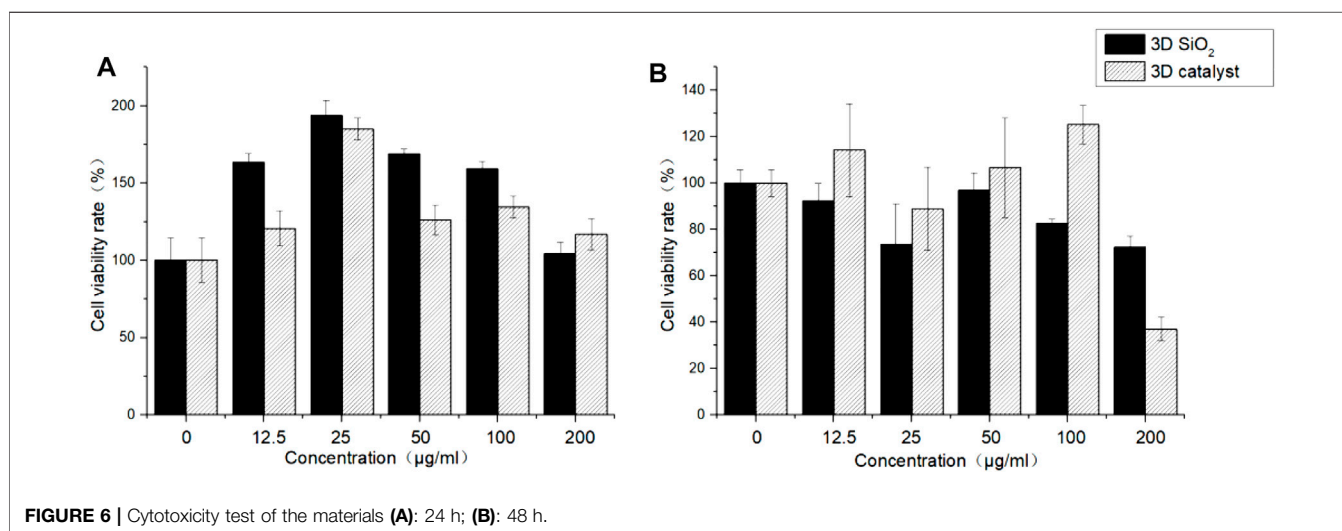
experiments. All reaction products were detected by thin-layer chromatography (TLC) per 5 min. **Table 2** shows that the reaction either did not take place or was minimal in the absence of catalyst material (Entry 3) or in the presence of 3D SiO$_2$ (Entry 4), respectively. However, high reaction yields were obtained in 20 min with both porous catalysts (Entries 1 and 2). Of the two materials, 3D SiO$_2$-NH-SO$_3$H exhibited a better catalytic effect, with a 96% yield, which may be due to the presence of more sulfonic acid groups compared to 3D SiO$_2$-SO$_3$H (**Table 2**).

To gain a deeper understanding of the materials' effect in protecting a series of alcohols, various alcohols were reacted with 3, 4-dihydro-2*H*-pyran in the presence of 3D SiO$_2$-NH-SO$_3$H. Catalytic reaction products were characterized by FTIR and 1H NMR spectroscopy (see **Supplementary Material**). The experiment showed that the porous silica-

model construction *in vitro* to evaluate the potential influence of different factors.

CONCLUSION

Some achievements have been obtained in bone and cartilage repair including clinical trial and applications when using 3D printing as an efficient tool to control the accurate microstructure of the scaffold in tissue engineering. However, the cure rate still remains a problem due to the complicated situation of the *in vivo* physiological environment, especially the microenvironment surrounding the damaged site. To study the influence of the microenvironment, a catalytic strategy was proposed to eliminate the residue of the scaffold degradation segment. In addition, an *in vitro* model will provide a simple and

practical platform to evaluate these changes. Therefore, a porous silica-based solid-acid catalyst material was successfully prepared by additive manufacturing technology and the results showed excellent catalytic performance. The catalytic strategy by constructing an *in vitro* model supplies an alternative way in environment evaluation of osteochondral repair and it also shows potential for the enzymatic catalytic research during the body's metabolism process in the future studies.

DATA AVAILABILITY STATEMENT

The original contributions presented in the study are included in the article/**Supplementary Material**, further inquiries can be directed to the corresponding author.

AUTHOR CONTRIBUTIONS

All authors contributed significantly to this work. YL, RL and SW conceptualized the system and designed the studies. YJ performed the experiments with assistance from JG, GR, XG, XX, YW, RY and ZL. RL, JG and GR performed the experiments for the revision. YJ wrote the draft and finished the manuscript with assistance from YL for revision. RL wrote the revision.

FUNDING

SUPPLEMENTARY MATERIAL

The Supplementary Material for this article can be found online at: https://www.frontiersin.org/articles/10.3389/fbioe.2021.790139/full#supplementary-material

REFERENCES

Azzena, U., Carraro, M., Modugno, G., Pisano, L., and Urtis, L. (2018). Heterogeneous Acidic Catalysts for the Tetrahydropyranylation of Alcohols and Phenols in green Ethereal Solvents. *Beilstein J. Org. Chem.* 14, 1655–1659. doi:10.3762/bjoc.14.141

Díaz-Marta, A. S., Tubio, C. R., Carbajales, C., Fernández, C., and Coelho, A. (2018). Three Dimensional Printing in Catalysis: Combining 3D Heterogeneous Copper and Palladium Catalysts for Multicatalytic Multicomponent Reactions. *ACS Catal.* 8, 392–404. doi:10.1021/acscatal.7b02592

Du, Y., Ge, J., Shao, Y., Ma, P. X., Chen, X., and Lei, B. (2015). Development of Silica Grafted Poly(1,8-Octanediol-Co-Citrates) Hybrid Elastomers with Highly Tunable Mechanical Properties and Biocompatibility. *J. Mater. Chem. B* 3, 2986–3000. doi:10.1039/c4tb02089h

Hopkins, T., Wright, K. T., Kuiper, N. J., Roberts, S., Jermin, P., Gallacher, P., et al. (2021). An *In Vitro* System to Study the Effect of Subchondral Bone Health on Articular Cartilage Repair in Humans. *Cells* 10, 1903. doi:10.3390/cells10081903

Ishikawa, S., Iijima, K., Sasaki, K., Hashizume, M., Kawabe, M., and Otsuka, H. (2018). Cartilage Differentiation of Bone Marrow-Derived Mesenchymal Stem Cells in Three-Dimensional Silica Nonwoven Fabrics. *Appl. Sci.* 8, 1398. doi:10.3390/app8081398

Kamble, R., Gaikwad, M., Tapare, M., Hese, S., Kadam, S., Ambhore, A., et al. (2021). DTP/SiO2: an Efficient and Reusable Heterogeneous Catalyst for Synthesis of Dihydropyrano[3,2-C]chromene-3-Carbonitrile Derivatives. *J. Appl. Organomet. Chem.* 1, 22–28. doi:10.22034/JAOC.2021.276239.1004

Khder, A. E. R. S., Ahmed, S. A., Khairou, K. S., and Altass, H. M. (2018). Competent, Selective and High Yield of 7-Hydroxy-4-Methyl Coumarin over Sulfonated Mesoporous Silica as Solid Acid Catalysts. *J. Porous Mater.* 25, 1–13. doi:10.1007/s10934-017-0414-1

Kumar, B., Aga, M. A., Rouf, A., Shah, B. A., and Taneja, S. C. (2014). Tetrahydropyranyl Ether (THPE) Formation in Hydroxyl Group protection and Conversion to Other Useful Functionalities. *RSC Adv.* 4, 21121–21130. doi:10.1039/c4ra02093f

Li, S., Tallia, F., Mohammed, A. A., Stevens, M. M., and Jones, J. R. (2000). Scaffold Channel Size Influences Stem Cell Differentiation Pathway in 3-D Printed Silica Hybrid Scaffolds for Cartilage Regeneration. *Biomater. Sci.* 8, 4458–4466. doi:10.1039/c9bm01829h

Li, X., Bian, S., Zhao, M., Han, X., Liang, J., Wang, K., et al. (2021). Stimuli-responsive Biphenyl-Tripeptide Supramolecular Hydrogels as Biomimetic Extracellular Matrix Scaffolds for Cartilage Tissue Engineering. *Acta Biomater.* 131, 128–137. doi:10.1016/j.actbio.2021.07.007

Ludwig, T., Seckendorff, J., Troll, C., Fischer, R., Tonigold, M., Rieger, B., et al. (2018). Additive Manufacturing of Al 2 O 3 -Based Carriers for Heterogeneous Catalysis. *Chem. Ingenieur Technik* 90, 703–707. doi:10.1002/cite.201700151

Nakhaei, A., Davoodnia, A., and Nakhaei, H. (2019). (NH4)42 [MoVl72MoV60O372(CH3COO)30(H2O)72] as a Heterogeneous Reusable Catalyst for Organic Reactions: Mini-Review. *J. Chem. Rev.* 1, 139–153. doi:10.33945/SAMI/JCR.2019.2.5

Narender, N., Suresh Kumar Reddy, K., Arun Kumar, M., Rohitha, C. N., and Kulkarni, S. J. (2010). Tetrahydropyranylation of Alcohols over Modified Zeolites. *Catal. Lett.* 134, 175–178. doi:10.1007/s10562-009-0205-7

Nelson, M., Li, S., Page, S. J., Shi, X., Lee, P. D., Stevens, M. M., et al. (2021). 3D Printed Silica-Gelatin Hybrid Scaffolds of Specific Channel Sizes Promote Collagen Type II, Sox9 and Aggrecan Production from Chondrocytes. *Mater. Sci. Eng. C* 123, 111964. doi:10.1016/j.msec.2021.111964

Niknam, K., Saberi, D., Sadegheyan, M., and Deris, A. (2010). Silica-bonded S-Sulfonic Acid: an Efficient and Recyclable Solid Acid Catalyst for the Synthesis of 4,4′-(arylmethylene)bis(1H-Pyrazol-5-Ols). *Tetrahedron Lett.* 51, 692–694. doi:10.1016/j.tetlet.2009.11.114

Pourghasemi-Lati, M., Shirini, F., Alinia-Asli, M., and Rezvani, M. A. (2018). Butane-1-sulfonic Acid Immobilized on Magnetic Fe3O4@SiO2nanoparticles: A Novel and Heterogeneous Catalyst for the One-Pot Synthesis of Barbituric Acid and Pyrano[2,3-D] Pyrimidine Derivatives in Aqueous media. *Appl. Organometal Chem.* 32, e4455. doi:10.1002/aoc.4455

Rafael, P., Celia, A., and Jesús, I. (2001). Synthesis of Enantiopure Mono- and Disubstituted Tetrahydroisoquinolines by 6-exo Radical Cyclizations. *Tetrahedron* 57, 4005–4014. doi:10.1016/S0040-4020(01)00274-5

Rajkumari, K., Kalita, J., Das, D., and Rokhum, S. L. (2017). Magnetic Fe3O4@silica Sulfuric Acid Nanoparticles Promoted Regioselective protection/deprotection of Alcohols with Dihydropyran under Solvent-free Conditions. *RSC Adv.* 7, 56559–56565. doi:10.1039/c7ra12458a

Ravindranath, N., Ramesh, C., and Das, B. (2001). Simple, Facile and Highly Selective Tetrahydropyranylation of Alcohols Using Silica Chloride. *Synlett* 2001, 1777–1778. doi:10.1055/s-2001-18078

Sajjadifar, S., Hamidi, H., and Pal, K. (2019). Revisiting of boron Sulfonic Acid Applications in Organic Synthesis: Mini-Review. *J. Chem. Rev.* 1, 35–46. doi:10.33945/SAMI/JCR.2019.1.3546

Shimizu, K.-i., Hayashi, E., Hatamachi, T., Kodama, T., and Kitayama, Y. (2004). SO3H-functionalized Silica for Acetalization of Carbonyl Compounds with Methanol and Tetrahydropyranylation of Alcohols. *Tetrahedron Lett.* 45, 5135–5138. doi:10.1016/j.tetlet.2004.04.186

Shin, H. S., Opanasenko, M., Cabello, C. P., Ryoo, R., and Čejka, J. (2017). Surfactant-directed Mesoporous Zeolites with Enhanced Catalytic Activity in Tetrahydropyranylation of Alcohols: Effect of Framework Type and Morphology. *Appl. Catal. A: Gen.* 537, 24–32. doi:10.1016/j.apcata.2017.02.019

Singh, Y. P., Moses, J. C., Bhardwaj, N., and Mandal, B. B. (2021). Overcoming the Dependence on Animal Models for Osteoarthritis Therapeutics - the Promises and Prospects of *In Vitro* Models. *Adv. Healthc. Mater.* 10, 2100961. doi:10.1002/adhm.202100961

Stuecker, J. N., Miller, J. E., Ferrizz, R. E., Mudd, J. E., and Cesarano, J. (2004). Advanced Support Structures for Enhanced Catalytic Activity. *Ind. Eng. Chem. Res.* 43, 51–55. doi:10.1021/ie030291v

Wang, C., Huang, W., Zhou, Y., He, L., He, Z., Chen, Z., et al. (2020). 3D Printing of Bone Tissue Engineering Scaffolds. *Bioactive Mater.* 5, 82–91. doi:10.1016/j.bioactmat.2020.01.004

Wei, P., Xu, Y., Zhang, H., and Wang, L. (2021b). Continued Sustained Insulin-Releasing PLGA Nanoparticles Modified 3D-Printed PCL Composite Scaffolds for Osteochondral Repair. *Chem. Eng. J.* 422, 130051. doi:10.1016/j.cej.2021.130051

Wei, W., Ma, Y., Yao, X., Zhou, W., Wang, X., Li, C., et al. (2021a). Advanced Hydrogels for the Repair of Cartilage Defects and Regeneration. *Bioactive Mater.* 6, 998–1011. doi:10.1016/j.bioactmat.2020.09.030

Williams, D. B. G., Simelane, S. B., Lawton, M., and Kinfe, H. H. (2010). Efficient Tetrahydropyranyl and Tetrahydrofuranyl protection/deprotection of Alcohols and Phenols with Al(OTf)3 as Catalyst. *Tetrahedron* 66, 4573–4576. doi:10.1016/j.tet.2010.04.053

Xing, J., Peng, X., Li, A., Chen, M., Ding, Y., Xu, X., et al. (2021). Gellan Gum/alginate-Based Ca-Enriched Acellular Bilayer Hydrogel with Robust Interface Bonding for Effective Osteochondral Repair. *Carbohydr. Polym.* 270, 118382. doi:10.1016/j.carbpol.2021.118382

Xintong, Z., and Chang-jun, L. (2017). Three-dimensional Printing for Catalytic Applications: Current Status and Perspectives. *Adv. Funct. Mater.* 27, 1701134. doi:10.1002/adfm.201701134

Xue, X., Hu, Y., Deng, Y., and Su, J. (2021). Recent Advances in Design of Functional Biocompatible Hydrogels for Bone Tissue Engineering. *Adv. Funct. Mater.* 31, 2009432. doi:10.1002/adfm.202009432

Yu, Y., Yu, X., Tian, D., Yu, A., and Wan, Y. (2021). Thermo-responsive Chitosan/silk Fibroin/amino-Functionalized Mesoporous Silica Hydrogels with strong and Elastic Characteristics for Bone Tissue Engineering. *Int. J. Biol. Macromolecules* 182, 1746–1758. doi:10.1016/j.ijbiomac.2021.05.166